Published in final edited form as:
J Neurochem. 2008 December ; 107(5): 1236–1247. doi:10.1111/j.1471-4159.2008.05695.x.

Impairment of nigrostriatal dopamine neurotransmission by manganese is mediated by pre-synaptic mechanism(s): Implications to manganese-induced parkinsonism

Tomás R. Guilarte[1,*], **Neal C. Burton**[1], **Jennifer L. McGlothan**[1], **Tatyana Verina**[1], **Yun Zhou**[3], **Mohab Alexander**[3], **Luu Pham**[2], **Michael Griswold**[2], **Dean F. Wong**[3], **Tore Syversen**[4], and **Jay S. Schneider**[5]

[1]Department of Environmental Health Sciences, Johns Hopkins University Bloomberg School of Public Health, Baltimore, MD, USA.

[2]Department of Biostatistics, Johns Hopkins University Bloomberg School of Public Health, Baltimore, MD, USA.

[3]Department of Radiology, Johns Hopkins Hospital, Baltimore, MD, USA.

[4]Department of Neuroscience, Norwegian University of Science and Technology, Trondheim, Norway.

[5]Department of Pathology, Anatomy and Cell Biology, Thomas Jefferson University, Philadelphia, PA, USA.

Abstract

The long-term consequences of chronic manganese (Mn) exposure on neurological health is a topic of great concern to occupationally-exposed workers and in populations exposed to moderate levels of Mn. We have performed a comprehensive assessment of Mn effects on dopamine (DA) synapse markers using Positron Emission Tomography (PET) in the non-human primate brain. Young male *Cynomolgus macaques* were given weekly i.v. injections of 3.3-5.0 mg Mn/kg (n=4), 5.0-6.7 mg Mn/kg (n=5), or 8.3-10.0 mg Mn/kg (n=3) for 7-59 weeks and received PET studies of various DA synapse markers before (baseline) and at one or two time points during the course of Mn exposure. We report that amphetamine-induced DA release measured by PET is markedly impaired in the striatum of Mn-exposed animals. The effect of Mn on DA release was present in the absence of changes in markers of dopamine terminal integrity determined in *post-mortem* brain tissue from the same animals. These findings provide compelling evidence that the effects of Mn on DA synapses in the striatum are mediated by inhibition of DA neurotransmission and are responsible for the motor deficits documented in these animals.

Keywords

manganese; dopamine release; Positron Emission Tomography; parkinsonism; non-human primate; striatum

[*]Corresponding author: Neurotoxicology & Molecular Imaging Laboratory Department of Environmental Health Sciences Johns Hopkins Bloomberg School of Public Health 615 North Wolfe Street, Room E6622 Baltimore, Maryland 21205 Phone: 410-955-2485 FAX: 410-502-2470 tguilart@jhsph.edu.

Introduction

Exposure to high concentrations of manganese (Mn) produces a debilitating neurological syndrome called manganism. The clinical manifestation of manganism includes early psychiatric symptoms and cognitive deficits followed by movement abnormalities resembling idiopathic Parkinson's disease (IPD). The description of parkinsonism resulting from occupational exposures to high levels of Mn can be traced to the original report by Couper (1837). Since then, many studies of workers occupationally exposed to moderate concentrations of Mn have confirmed an atypical form of parkinsonism (see review by Olanow, 2004). Additional support for parkinsonism resulting from increased concentrations of Mn in the brain comes from patients with medical conditions related to liver disease (Fabiani et al. 2007;Hauser et al. 1994) in which the biliary excretion of Mn is impaired and brain Mn concentrations increase (Butterworth et al. 1995), patients receiving high levels of Mn from parenteral nutrition (Iinuma et al. 2003) and from drug addicts injecting psychostimulant drugs containing high concentrations of Mn (Meral et al. 2007;Stepens et al. 2008). Lastly, recent studies suggest that exposure to ambient levels of Mn generated from gasoline containing the Mn additive methylcyclopentadienyl manganese tricarbonyl (MMT) (Finkelstein and Jerrett 2007) industrial emissions (Rodriguez-Agudelo et al. 2006;Lucchini et al. 2007) and welding (Racette et al. 2001;Racette et al. 2005) may be associated with an increased prevalence of movement abnormalities and parkinsonism.

The clinical expression of Mn-induced parkinsonism includes gait disturbances with bradykinesia, frequent falls, rigidity, micrographia, masked facies, and 'cock-gait.' (Cersosimo and Koller 2006). Although some of these symptoms are similar to IPD, other symptoms are different. For example, dystonia and dyskinesia with postural instability and action tremor and little or no resting tremor is more frequently observed in Mn-induced parkinsonism. In IPD, unilateral resting tremor is often but not always seen as an early clinical sign of disease expression that is not present in Mn-induced parkinsonism. Lastly, the restoration of dopamine (DA) levels in the striatum by L-DOPA therapy is the mainstay therapy in IPD while this approach is generally ineffective in alleviating the symptoms of Mn-induced parkinsonism (Lu et al. 1994). The differences in clinical presentation and in the response to L-DOPA therapy clearly indicate that IPD and Mn-induced parkinsonism are different in their pathophysiology.

Neuropathological examination of brain tissue also supports significant differences between IPD and Mn-induced parkinsonism. In IPD, there is unequivocal evidence from neuropathological and neuroimaging studies that dopaminergic neurons whose cell bodies are located in the substantia nigra pars compacta (SNpc) exhibit an age-dependent progressive retrograde degeneration leading to the loss of axon terminals in the striatum (caudate and putamen) resulting in a profound deficit in striatal DA concentrations and culminating in the loss of DA cell bodies. The deficit in striatal DA concentrations is responsible for the movement abnormalities that are typical of IPD. A recent review of the available literature indicates a limited number of neuropathological studies in humans chronically exposed to Mn (Perl and Olanow 2007). From this limited number of autopsy specimens, there is evidence of Mn-induced degeneration in basal ganglia structures such as the globus pallidus and subthalamic nucleus with little or no involvement of the SNpc (Yamada et al. 1986;Bernheimer et al. 1973). There is one case report of an individual with occupational Mn exposure that expressed neuronal loss in the SNpc and the presence of Lewy bodies (Bernheimer et al. 1973). Lewy bodies are a hallmark feature in the pathology of IPD. However, one cannot eliminate the possibility that this was a case of IPD with coincidental occupational Mn exposure.

The neuropathological basis of Mn-induced parkinsonism has also been investigated in a limited number of non-human primate studies. For the most part, these studies have provided conflicting results since in some cases they have found decreased DA concentrations in the striatum with no pathological involvement of the SNpc (Perl and Olanow 2007). Neuropathological studies in non-human primates do support involvement of other basal ganglia structures such as the globus pallidus and subthalamic nuclei as documented in human cases. Despite these investigations there are lingering questions related to the Mn dose and duration of exposure necessary to produce changes in DA synapses as well as the neuroanatomical site(s) and neurotransmitter system(s) responsible for Mn-induced parkinsonism. A resolution to this long-standing question has significant implications to the clinical management of Mn-exposed individuals, to the derivation of novel therapeutic strategies and to the revision of Mn exposure limits in the work environment and for the general population.

Molecular Imaging techniques such as Positron Emission Tomography (PET) and Single Photon Emission Computed Tomography (SPECT) have provided valuable information in understanding the biochemical changes at nigrostriatal dopaminergic synapses in subjects with IPD. In Mn-induced parkinsonism, there is suggestive evidence from PET and SPECT studies of changes in some dopaminergic synapse markers. Studies performed in workers who are both occupationally exposed to Mn and express movement abnormalities suggest that these individuals have normal [^{18}F]-DOPA PET scans indicative of an intact nigrostriatal dopaminergic system (Shinotoh et al. 1997;Wolters et al. 1989) (but see Racette et al. 2005). The study by Wolters et al. (1989) also found a slight reduction in D2-dopamine receptors (D2R) levels measured by [^{11}C]-raclopride PET. Based on these findings, it has been suggested that Mn-induced parkinsonism is not mediated by degeneration of nigrostriatal DA neurons but by changes in post-synaptic dopaminergic signaling intrinsic to the caudate/putamen and/or its connections to the globus pallidus. More recently, SPECT studies have assessed DAT levels in the striatum of individuals with elevated levels of Mn in the basal ganglia. These studies have been case reports of Mn-exposed subjects and there is evidence of changes in DAT levels in the striatum (Huang et al. 2003;Kim et al. 2002). However, other studies have not supported such findings (Kim et al. 2007). The significance of alterations in DAT levels in Mn-exposed subjects measured by SPECT is difficult to interpret in the absence of other evidence that they may represent DA terminal degeneration since reduction in DAT may represent degeneration of terminals, down-regulation of DAT protein or inhibition of the ligand-DAT interaction by Mn. Molecular imaging studies in Mn-exposed non-human primates have also described changes in D2R and DAT levels (Eriksson et al. 1992;Chen et al. 2006). However, the significance or molecular mechanism(s) by which chronic exposure to Mn produces changes in DA synapse markers and results in movement abnormalities has remained elusive and controversial.

We have recently reported using PET imaging that monkeys chronically exposed to 3.3-5.0 mg Mn/kg once per week for approximately 10 months expressed a marked decrease of amphetamine-induced DA release (AMPH-DAR) in the striatum (Guilarte et al. 2006a). Chronic Mn exposure in these animals did not affect DAT or D2R levels in the striatum measured by PET. Therefore, it appeared that AMPH-DAR was the most sensitive DA synapse marker affected by chronic Mn exposure. Further, decreased AMPH-DAR was associated with subtle deficits in fine motor control and hypoactivity (Guilarte et al. 2006a;Schneider et al. 2006). Consistent with the PET findings, analysis of *post-mortem* brain tissue from the same animals showed no significant effect of chronic Mn exposure on striatal DA concentrations or in DAT and D2R levels. Tyrosine hydroxylase (TH) immunohistochemistry confirmed that DA presynaptic terminals in the striatum were intact in these Mn-exposed non-human primates (Guilarte et al. 2006a). Taken together, these findings indicated an intact but dysfunctional nigrostriatal DA system in the non-human

primate striatum. As a continuation of these preliminary studies, we now have additional monkeys that have been administered higher doses of Mn per week and have undergone similar behavioral and molecular imaging studies as well as neuropathological examination of *post-mortem* brain tissue. Importantly, we also included two control animals that received the same series of behavioral and imaging studies without exposure to Mn. This report is a summary of the largest cohort of Mn-exposed non-human primates that have been studied to date using behavioral, neuroimaging and neuropathological endpoints to assess the effects of chronic Mn exposure. Our findings provide strong support to the hypothesis that Mn-induced changes on nigrostriatal DA synapses are most likely mediated by pre-synaptic mechanisms that lead to marked inhibition of DA release and this effect mediates changes in motor function that are typical of chronic Mn exposure.

Materials and Methods

Manganese administration and husbandry

Adult male research naïve *Cynomolgus macaques* (five to six years of age at the start of the study and housed at Thomas Jefferson University) were used. All animal studies were reviewed and approved by the Johns Hopkins and the Thomas Jefferson University Animal Care and Use Committees. In this report, we have combined data from all animals that have been exposed to Mn and received neuroimaging studies including those that have already been described in a preliminary communication (Guilarte et al. 2006a). In this previous report, we described animals that were administered Mn at a dose of 3.3-5.0 mg Mn/kg body weight once per week (Guilarte et al. 2006a). When we started to administer higher doses of Mn per body weight, we learned that the animals did not tolerate higher doses well; therefore, we changed the Mn administration protocol by administering one half of the weekly Mn dose on two different occasions per week rather than once weekly. This change in the Mn administration protocol was well tolerated by all of the animals. The dose level and cumulative Mn dose for all Mn-exposed animals that received neuroimaging studies are provided in Table 1. In this study, we also included two animals that received the same behavioral and neuroimaging studies as the Mn-exposed animals but received no Mn as a separate control group. These animals are called “imaged-controls” to distinguish them from naïve controls that did not receive the neuroimaging studies or Mn.

The paradigm for Mn administration has been described previously (Schneider et al. 2006;Guilarte et al. 2006a;Guilarte et al. 2006b). Animals received the same series of PET imaging studies at baseline (prior to Mn administration) and at two different time points during the Mn administration defined as Mn-1 (first imaging set after initiation of Mn administration) and Mn-2 (second imaging set after initiation of Mn administration). At the end of the PET studies, animals were euthanized by ketamine injection (20-30 mg/kg) followed by an overdose of pentobarbital (100 mg/kg) and the brain harvested for *post-mortem* studies. The brain was immediately immersed in warm low-boiling point agarose and sliced in 4 mm slabs from which one hemisphere was maintained frozen at −80°C and the slab from the opposite hemisphere was post-fixed for immunohistochemistry studies and kept at −80°C.

Positron Emission Tomography (PET) Imaging and Quantification

General PET imaging protocols have been described by us previously (Guilarte et al. 2006a;Chen et al. 2008). [^{11}C]-methylphenidate PET for DAT and [^{11}C]-raclopride with amphetamine (AMPH) challenge PET for AMPH-induced DA release (AMPH-DAR) and D2R measurements were performed on the same day for each animal. The [^{11}C]-methylphenidate PET scan was always done first followed by the [^{11}C]-raclopride with AMPH challenge PET scan. For AMPH-DAR release and D2R binding potential (BP),

animals were studied with a bolus plus continuous infusion method (Bolus/Infusion ratio=75) using the D2R ligand [^{11}C]-raclopride as described (Guilarte et al. 2006a;Zhou et al. 2006). All monkeys received a continuous infusion of [^{11}C]-raclopride over a 90-minute scanning period with AMPH (2.0 mg/kg IV) delivered at 40 minutes from the onset of [^{11}C]-raclopride infusion. The change in [^{11}C]-raclopride binding following AMPH was measured and used to infer the magnitude of DA release. D2R BP was estimated from the first 0-40 min of the [^{11}C]-raclopride time-activity curves (TACs) prior to AMPH-administration. For each PET study, regions of interest were drawn on multiple slices encompassing the left and right striata and the cerebellum. Time-activity curves were generated for each region. A simplified reference tissue model (SRTM) with cerebellum as reference tissue was used to estimate BP of [^{11}C]-methylphendiate (Lammertsma and Hume 1996).

Manganese concentration in blood and brain tissue measured by high-resolution inductively-coupled plasma mass spectrometry (HR-ICP-MS)

Blood and brain samples were analyzed for metal content by HR-ICP-MS using a Thermo (Finnigan) model Element 2 instrument (Bremen, Germany) as previously described (Guilarte et al. 2006a).

Quantitative autoradiography

Fresh frozen tissue slabs at the level of the caudate/putamen were sectioned at 20 μm on a freezing cryostat (Leica, Nussloch, Germany) in the coronal plane, thaw-mounted on 50 × 75 × 1.0 mm adhesion superfrost plus slides (Brain Research Laboratories, Newton, MA, USA) and stored at −80°C until use.

Dopamine transporters—[^{125}I]-RTI-121 autoradiography was performed to measure DAT levels as previously described (Strazielle et al. 1998). Briefly, slides were pre-washed for 30 min and incubated in 50 mM Tris–HCl (pH 7.4) with 26 pM [^{125}I]-RTI-121 (2200 Ci/mmol, Perkin-Elmer) for 60 min at 25 °C. Non-specific binding was assessed in adjacent sections by adding a final concentration of 10 μM unlabeled GBR12909 (Sigma). Tissue was washed in buffer, air dried and apposed to KODAK BioMax MR film, MR-1, along with [^{125}I]-Microscales (Amersham) for 21 h. Autoradiography was conducted using slides of coronal brain sections of the rostral caudate/putamen (Bregma, 3.60 mm). A rhesus monkey brain atlas was used to define distinct brain areas (Paxinos et al. 2000).

Vesicular monoamine transporter type-2 (VMAT2)—Slides were pre-washed in 20 mmol/L HEPES, 300 mmol/L sucrose buffer (pH 8.0) for 15 min at 22–24°C. Slides were incubated at 22–24°C for 60 min in buffer with 3.0 nmol/L [^{3}H]-alpha-dihydrotetrabenazine (DTBZ) (specific activity: 740 GBq/mmol or 20 Ci/mmol) (ARC; American Radiolabeled Chemicals Inc., St Louis, MO, USA) to determine total binding. Non-specific binding was determined in adjacent brain slices with 2 μmol/L non-radioactive DTBZ (American Radiolabeled Chemicals). Slides were then rinsed three times at 22–24°C in 40 mmol/L HEPES, 32 mmol/L sucrose buffer (pH 8.0) for 5 min each followed by a rinse in dH_2O at 4°C and dried under a stream of cool air. Slides were apposed to Kodak Bio-Max MR films for 8 weeks at 22–24°C. Autoradiography was conducted using slides of coronal brain sections of the rostral caudate/putamen (Bregma, 3.60 mm).

Dopamine D2 Receptors (D2R)—Slides were pre-washed in 50 mM Tris buffer (pH 7.1) containing 120 mM NaCl, 5 mM KCl, 2 mM CaCl2, 1 mM MgCl2 for 5 minutes at 36°C. Total binding was determined by incubating slides at 36°C for 30 minutes in the same buffer containing 40 nM ketanserin to block the binding of the tracer to serotonergic receptors and 1.4 nM [3H]-spiperone (specific activity: 15 Ci/mmol, Perkin Elmer Life and

Analytical Sciences, Boston, MA). Non-specific binding was determined in adjacent brain slices incubated in the presence of 1 μM (+)-butaclamol (Sigma, St. Louis, MO). After 3 rapid washes in buffer at 0°C, followed by a rinse in ice cold dH2O, slides were dried at 37°C for 1 hour and left to dry at room temperature overnight. Slides were apposed to Kodak Bio-Max MR films for 6-7 weeks at 22–24°C. Autoradiography was conducted using slides of coronal brain sections of the rostral caudate/putamen (Bregma, 3.60 mm).

Dopamine D1 receptors (D1R)—A modification of a previously established protocol (Sari et al. 2006) was used to visualize and measure the distribution of D1 receptors. Frozen sections were thawed on a slide warmer for 30 minutes at 37°C. The slides were then pre-incubated for 20 minutes in 25°C buffer (50 mM Tris HCl, pH 7.4 with 120 mM NaCl, 5 mM KCl, 2 mM $CaCl_2$, and 1 mM $MgCl_2$). D1 receptors were then labeled with 25°C 1 nM [^{3}H]-SCH23390 (specific activity: 85.0 Ci/mmol; Perkin Elmer) for 30 minutes. Non-specific binding was assessed in adjacent sections with the addition of non-radioactive 5 μM (+)-butaclamol. Sections were then rinsed five times in buffer at 4°C for 20 seconds each. The slides were then dipped in dH2O, and dried under a stream of cool air. Autoradiography was conducted using slides of coronal brain sections of the rostral caudate/putamen (Bregma, 3.60 mm).

Cannabinoid receptor 1 (CB1)—Cannabinoid receptor binding was performed as described by (Newell et al. 2006). Briefly, sections were pre-incubated with 50 mM Tris-HCl (pH 7.4) containing 5% bovine serum albumin (BSA) for 30 min at room temperature. Sections were then incubated with 8.4 nM [^{3}H]-CP-55940 (specific activity: 139.6 Ci/mmol, Perkin Elmer) for 2 hr at room temperature. Non-specific binding was determined by incubating adjacent sections in 8.4 nM [^{3}H]-CP-55940 in the presence of 10 μM CP-55940. Following incubation, sections were washed three times: first in 50 mM Tris-HCl (pH 7.4) containing 1% BSA for 1 hr at 4°C; the second wash was in 50 mM Tris-HCl (pH 7.4) for 3 hr at 4°C; and, the third wash was in the same buffer for 5 min at 4°C. Finally, sections were dipped in distilled water and air-dried. Slides were apposed to Kodak Bio-Max MR films for 4 weeks. Autoradiography was conducted using slides of coronal brain sections of the caudal caudate/putamen at the level of the globus pallidus (Bregma, −6.75 mm).

In all quantitative receptor autoradiography studies, reference [^{3}H]- or [^{125}I]-microscales standards (Amersham, Arlington Heights, IL, USA) were included with each film to ensure linearity of optical density and to allow quantitative analysis of the images. Images from autoradiograms were captured using an image analysis system (Loats Associates Inc., Westminster, MD, USA) and densitometric analysis was performed using NIH Image v1.63.

Analysis of dopamine and metabolites in post-mortem brain tissue

Caudate and putamen samples were assayed for DA and its metabolites homovallinic acid (HVA) and dihydroxyphenylacetic acid (DOPAC) using a HPLC (Shimadzu North America, Columbia, MD, USA) with electrochemical detection system (ESA Coulochem III ECD, ESA Inc., Chelmsford, MA, USA). Each sample was assayed according to a previously described protocol (Guilarte et al. 1987) with the modification that a commercially available mobile phase was used (MDTM-70-1332; ESA Labs, Chelmsford, MA) Briefly, tissue was sonicated in 10 volumes of 0.1 mol/L perchloric acid and the homogenate was centrifuged at 7400 × *g* for 15 min and the resulting supernatant was filtered through Phenex 4 mm non-sterile 0.2 μm nylon syringe filters. Twenty microliters of the filtered supernatant (1:1 dilution for controls) was injected into a 5 μm C18 (4.6 × 150 mm) reverse-phase column with a flow rate of 0.6 mL/min. Monoamine detection occurred with a guard potential of +0.35 V, with channel one potential of the analytical cell set to −0.15 V and channel two potential set to +0.22 V, each channel with a sensitivity of 1 μA. Integration of the peaks

was performed using LC Solution software (Shimadzu, Columbia, MD). The concentration of individual samples was calculated using a line of best fit ($R^2 > 0.99$) from the injected standards (0.1–8 μg/mL).

Tyrosine Hydroxylase (TH) and DAT immunohistochemistry

We used standard immunohistochemistry procedures with rabbit anti-TH (Chemicon, 1:2000, 48 hrs at 4°C) and rat anti-DAT antibodies (Chemicon, 1:2000) followed by avidin-biotinperoxydase reaction with 3,3′-diaminobenzidine. Images were acquired and optical densities measured using the MCID Core 7.0 (Interfocus Imaging, Linton, England).

Statistical Analysis

Assessments prior to and following Mn exposure were compared by repeated measures ANOVA. Pair-wise post-hoc comparisons were performed to assess changes between baseline and post-Mn observation periods. Statistical analysis of PET studies was performed using regression with clustering on animal to account for repeated measures on the same animal over time. Analysis of variance and Student's *t*-test were used where appropriate. Statistical significance was set at $p < 0.05$. All values are expressed as mean ± sem.

Results

Manganese concentrations in blood and brain tissue

Figure 1A shows the levels of Mn in blood at baseline and at the Mn-1 (124 ± 12 days) and Mn-2 (285 ± 13 days) time points. The figure shows that the average blood Mn concentrations were in the 65-85 μg/L range. This level of Mn exposure is within the upper range of blood Mn concentrations that have been documented in human populations such as those living near Mn mining areas (Santos-Burgoa et al. 2001), in mothers and newborns (Takser et al. 2003) and in children in communities in which MMT is used in gasoline (Gulson et al. 2006) and as a result of parenteral nutrition (Iinuma et al. 2003).

The concentration of Mn in various brain regions is provided in Figure 1B. The data shows that there were significant elevations in Mn concentrations in all brain regions from Mn-exposed animals relative to controls (Figure 1B). Consistent with what is known about Mn distribution in the human and non-human primate brain, the globus pallidus contained the highest accumulation of Mn relative to all other brain regions. The globus pallidus was followed by the putamen and caudate with frontal white matter and frontal cortex accumulating the lowest levels of Mn.

In vivo PET imaging and quantification

For the PET imaging studies, we have combined all of the animals that have gone through the entire imaging protocol and were exposed to Mn including the 4 Mn-exposed animals whose results have already been described in a preliminary communication (Guilarte et al. 2006a). Importantly, besides the naïve control animals (no Mn exposure or neuroimaging studies), two additional control animals that received the entire set of imaging studies but no Mn were also included. These two "imaged-control" animals signify an important control group in order to assess any effect that the repeated AMPH administration may have on subsequent PET studies since AMPH is used to stimulate DA release in the AMPH-DAR PET studies and could alter DA synaptic markers. Figure 2 depicts the results of the PET findings for all of the animals that received PET studies. This forms a total of 13 Mn-exposed animals and 2 imaged-controls. All Mn-exposed animals were pooled as a single group because statistical analysis indicated no significant differences for any of the PET markers amongst the three different Mn administration groups (delineated in Table 1). The data shows that AMPH-DAR is the most affected by chronic Mn exposure of the DA

synapse markers measured by PET. On average, there was a 36% decrease in AMPH-DAR at the Mn-1 time point (124 ± 12 days after initiation of Mn administration) and a 51% decrease at the Mn-2 time point (285 ± 13 days after initiation of Mn administration) relative to baseline. These changes in AMPH-DAR were significantly different from baseline but not from each other (Figure 2A). It is important to note that in the two "imaged-control" animals that received the same number of PET studies as the Mn-exposed animals, the level of AMPH-DAR did not change with time with the exception that at the Mn-2 time point, the value for one of the two animals increased. These findings clearly demonstrate that the highly significant decrease in AMPH-DAR was the result of the chronic Mn exposure. The current findings confirm and extend our preliminary report (Guilarte et al. 2006a) that chronic Mn exposure results in a marked inhibition of AMPH-DAR measured by PET.

We also measured a modest but significant decrease (19.5%) in DAT BP in the striatum at the Mn-1 time point and a 24.5% decrease at the Mn-2 time point relative to baseline values (Figure 2B). The decreases in DAT BP at both of the post-Mn time points were significantly different from baseline but not from each other. Finally, D2R BP expressed a small but non-significant decrease (9%) measured at the Mn-1 time point relative to baseline with a small but significant decrease (14.5%) at the Mn-2 time point relative to baseline (Figure 2C). No significant changes were measured between the Mn-1 and Mn-2 time points for D2R. When one compares the longitudinal DAT and D2R PET results obtained in the Mn-exposed animals to imaged-control animals, one can surmise that the longitudinal changes measured in the Mn-exposed animals for DAT can be accounted by procedural use of AMPH in the PET studies. The small effect of chronic Mn on D2R at the Mn-2 time point is not affected by AMPH administration (Figure 2C). Therefore, in general it appears that the greatest effect of chronic Mn exposure on the DA synapse is to decrease DA release.

Analysis of DA and metabolites in the caudate and putamen

Figure 3 shows the analysis of DA and its metabolites DOPAC and HVA in the caudate and putamen of control and Mn-exposed animals. The analysis of the data was performed based on three different control groups. We compared the effect of chronic Mn exposure to all control animals (naïve controls + imaged-controls), to naïve control animals only and to imaged-controls only. As noted, this was done since AMPH is administered for the AMPH-DAR studies and AMPH is a psychostimulant that interacts with DAT and it also stimulates DA release. The analysis indicates that when all control animals are combined, there were no significant differences between control and Mn-treated animals in regards to DA, DOPAC or HVA levels in the caudate and putamen (Figure 3A, 3B). When only naïve control animals were compared to Mn-exposed animals, we measured a significant decrease in DA and DOPAC levels in the putamen only with no effect on HVA concentrations (Figure 3B). Importantly, when the values from the Mn-exposed animals were compared to imaged-controls, the DA, DOPAC and HVA values (except for HVA in the putamen) for the Mn-exposed animals were always higher than the imaged-control group (Figure 3A, 3B). Further analysis of the ratio of DA to DOPAC (Figure 3C) shows that procedurally administered AMPH in imaged-controls decreases the turnover of DA. The ratio DA/DOPAC is consistent among groups in the caudate, and in the putamen only the imaged-controls have decreased ratios indicating that AMPH alters the turnover of DA. However, the Mn-exposed animals are not different from control in the caudate or putamen.

Quantitative autoradiography for DAT, VMAT2, D2R, D1R and CB1 in brain tissue

Post-mortem quantitative autoradiography of relevant DA transporters and receptors was performed in the brain of animals described in Table 1 and the results are presented in Figure 4. We also performed autoradiography for cannabinoid receptor 1 (CB1) (Figure 5) because these receptors are closely related to DA neurotransmission, are synthesized in

medium size spiny neurons in the caudate and putamen and are transported to efferent fibers projecting to the globus pallidus and substantia nigra pars reticulata (SNpr) where they are expressed at high concentrations (Julian et al. 2003). Statistical analysis of [^{125}I]-RTI-121 specific binding to DAT showed no significant effect of chronic Mn exposure when compared to all controls (Figure 4B). A significant decrease in [^{125}I]-RTI-121 specific binding was measured in the caudate and putamen when compared to naïve controls only. On the other hand, chronic Mn exposure produces an increased level of [^{125}I]-RTI-121 specific binding in Mn-exposed animals when compared to imaged-controls. This same pattern of differences between the different control groups and the Mn-treated animals was also observed for [^{3}H]-DTBZ binding to VMAT2 (see Figure 4D). Specific binding for [^{3}H]-spiperone to D2R was decreased in the Mn-exposed animals relative to the naïve controls. D2R levels in Mn-exposed animals were significantly reduced only in the putamen compared to naïve controls, while in the caudate the decrease in D2R in the Mn-exposed animals was near-significant. The observed effect on D2R was smaller than the effect observed on DAT or VMAT2 (see Figure 4B, 4D, and 4F). As with DAT and VMAT2 markers, the imaged-controls exhibited lower levels of D2R than the Mn-exposed animals. Analysis of specific binding for D1R and CB1 receptors demonstrated no significant effect of Mn exposure relative to any of the control groups (Figure 4H and Figure 5).

Tyrosine Hydroxylase (TH) and DAT immunohistochemistry as markers of dopamine neuronal terminal integrity

We performed immunohistochemistry for DAT and TH to examine protein levels as a different method of analysis of these DA synapse markers. Densitometry analysis of DAT in caudate and putamen did not reveal a significant effect of Mn-exposure (Figure 6A). However, there were lower levels of DAT in the imaged-control group relative to the Mn-exposed group confirming the effect of AMPH used in the AMPH-DAR PET studies on DAT. Tyrosine hydroxylase densitometry resulted in no significant effect of Mn-exposure relative to any of the control groups (Figure 6B). This finding clearly demonstrates that dopaminergic terminals are not degenerating in the caudate and putamen. The data also clearly shows that in the imaged-control animals, the procedural administration of AMPH affects all presynaptic markers measured, an effect that is not present in the Mn-exposed animals.

Discussion

The main finding of the present study is that chronic Mn administration produces a dramatic decrease of *in vivo* DA release and this effect is associated with motor function deficits. This large cohort of Mn-exposed non-human primates confirms and extends our preliminary report of Mn-induced dysfunction of the nigrostriatal DA system (Guilarte et al. 2006a). Importantly, the Mn-induced changes on DA release observed in the Mn-exposed animals were present in the absence of evidence of nigrostriatal DA terminal degeneration. However, it is important to recognize that the effects of Mn exposure described in this communication are the result of a relatively short exposure period and may represent early changes in dopamine synapses resulting from Mn exposure. A protracted exposure to Mn could produce other effects on the nigrostriatal DA system that may not be expressed in the amount of time in which our cohort of animals was assessed. The fact that Mn exposure markedly alters the function of nigrostriatal DA neurons by impairing DA release can have significant implications to changes in DA compartmentalization and generation of reactive oxygen species that in the long term could produce neuronal injury.

Previous investigations in which [^{18}F]-fluorodopa PET has been performed in workers occupationally exposed to Mn that exhibited parkinsonism demonstrated a normal PET scan indicative of an intact nigrostriatal dopaminergic system (Shinotoh et al. 1997;Wolters et al.

1989). Our present findings provide support to the notion that chronic Mn exposure within the length of time that the animals were exposed in the present study does not affect nigrostriatal DA neuron terminal integrity as TH levels did not change in the striatum of Mn-exposed animals. Largely as a result of the previous [^{18}F]-fluorodopa PET findings and earlier studies in which gross anatomical examination of the basal ganglia in a limited number of human and non-human brain autopsy specimens were done, the general dogma has been that Mn-induced parkinsonism is mediated by changes distal (post-synaptic) to the dopaminergic synapse (Olanow 2004). Our present findings do not support this interpretation since three markers that we have assessed that are localized to cells intrinsic to the caudate, putamen and globus pallidus (i.e., D1R, D2R and CB1 receptors) either expressed a very small change (D2R) or did not change (D1R, CB1) with Mn exposure. The most parsimonious interpretation of our results is that chronic Mn exposure produces motor function deficits by altering pre-synaptic DA terminal function resulting in a marked decrease in DA release impairing DAergic neurotransmission. This is consistent with the observation that one of the animals in the group receiving the highest weekly dose of Mn (animal #6697) that developed clinical signs of parkinsonism with severe dystonia and dyskinesias expressed the largest decline in AMPH-DAR from a baseline of 44% to 8.0% release measured by PET after only 7 weeks of Mn exposure. These findings indicate that Mn-induced motor function deficits are possible by mechanisms that inhibit DA release in the presence of normal levels of DA and an intact nigrostriatal DA system.

The present study also provides novel information about certain aspects of basal ganglia circuitry in Mn-exposed animals. Medium size spiny neurons (MSN) are the predominant cell type in the striatum (Surmeier et al. 2007). The prevailing opinion is that these neurons are segregated into two different pathways providing the major output of the striatum. The direct pathway that is largely composed of MSN expressing D1R, projects to the internal globus pallidus and substantia nigra pars reticulata (SNpr) while the indirect pathway with MSN containing D2R project to the external globus pallidus (Surmeier et al. 2007). In the striatum, D1R and D2R are primarily found in MSN dendrites, although D2R is also found presynaptically in DA terminals. Cannabinoid receptors (CB1) are presynaptically localized in striatonigral and striatopallidal terminals in the SNpr and globus pallidus, respectively (Julian et al. 2003). It is clear from our studies that Mn exposure does not alter D1R or CB1 receptors in the striatum or globus pallidus (Figure 4C and Figure 5). A small but significant decrease in D2R was measured by PET with cumulative Mn exposure suggesting that the level of this receptor may be affected. However, the effect of Mn on D2R levels was very small (14%) relative to the large group effect observed with Mn inhibition (50%) of DA release. These findings suggest that for the most part receptors at MSN projections are not affect by Mn exposure.

An important aspect of the present study was the addition of an “imaged-control” group in which the animals were subject to the same behavioral and neuroimaging studies as the Mn-exposed animals but did not receive Mn administration. This was a critically important control group in order to assess the potential effect that AMPH administration (used for the AMPH-DAR PET studies) may have on the various DA synapse markers as AMPH is known to alter DA, DAT and VMAT2 levels (Fleckenstein et al. 2007). Two observations can be made from comparing the imaged-control group to the Mn-exposed animals. First, it appears that the decrease in DAT BP measured by PET in the Mn-exposed animals is largely accounted for by the AMPH administered as the imaged-control animals expressed the same degree of longitudinal change in DAT BP as the Mn-exposed animals (Figure 2B). The AMPH administration, however, did not significantly affect D2R BP or AMPH-DAR. Secondly, from the *post-mortem* neurochemical measurements it appears that chronic Mn exposure may interfere with the effects of AMPH on dopaminergic synapse markers. This is based on the findings that striatal DA, DAT and VMAT2 levels in *post-mortem* tissue from

imaged-controls were lower than those for Mn-exposed animals suggesting that Mn partially blocks the known AMPH-induced decreases on these DA synapse markers. This observation is consistent with studies indicating that DAT inhibitors such as cocaine or GBR12909 reduce uptake of Mn in striatal tissue (Ingersoll et al. 1999;Anderson et al. 2007) and that Mn inhibits DA uptake in striatal synaptosomes (Chen et al. 2006;Anderson et al. 2007). These observations provide additional evidence that Mn directly interacts with DAT to alter AMPH effects on DA synapse markers.

The possibility that Mn may enter the DA terminal through DAT provides important insights on potential mechanism(s) by which Mn may inhibit DA release. That is, if Mn enters the DA neuronal terminal through DAT, it could interact with pre-synaptic proteins to alter pre-synaptic function. In this context, Mn has been shown to interact *in vitro* with α-synuclein to alter its conformation (Uversky et al. 2001). α-synuclein is a pre-synaptic cytosolic protein known to be associated with dopaminergic neurons from a physiological and pathological perspective (Wright and Brown 2008). A recently discovered function of α-synuclein is to assist in the folding and refolding of synaptic SNARE proteins that are essential for neurotransmitter release (Chandra et al. 2005). Thus, it is possible that the effect of Mn on DA release measured by PET as described in the present study may be mediated by Mn interacting with and altering the function of proteins that are essential for vesicular neurotransmitter release. An alternative or concurrent mechanism that may be operational is that Mn gains entry into DA neuron terminals via voltage-gated calcium channels (Narita et al. 1990). This mode of entry of Mn into neuronal terminals has been associated with inhibition of calcium-mediated exocytotic neurotransmitter release in the neuromuscular junction (Meiri and Rahamimoff 1972).

In summary, in this communication we describe the effects of chronic Mn exposure on the largest cohort of non-human primates ever studied using PET with extensive confirmation of *in vivo* PET findings using *ex vivo* neurochemical measurements in brain tissue from the same animals. Our results indicate that motor function abnormalities induced by Mn-exposure are likely mediated by inhibition of DA release in the striatum and shed new light on the molecular basis of Mn-induced parkinsonism.

Acknowledgments

Supported by NIEHS grant number ES010975 to TRG. NCB was supported by NIEHS training grant #T32 ES07141.

Reference List

Anderson JG, Cooney PT, Erikson KM. Inhibition of DAT function attenuates manganese accumulation in the globus pallidus. Environ Toxicol Pharmacol. 2007; 23:179–184. [PubMed: 17387379]

Bernheimer H, Birkmayer W, Hornykiewicz O, Jellinger K, Seitelberger F. Brain dopamine and the syndromes of Parkinson and Huntington. Clinical, morphological and neurochemical correlations. J Neurol Sci. 1973; 20:415–455. [PubMed: 4272516]

Brucke T, Asenbaum S, Pirker W, Djamshidian S, Wenger S, Wober C, Muller C, Podreka I. Measurement of the dopaminergic degeneration in Parkinson's disease with [^{123}I] beta-CIT and SPECT. Correlation with clinical findings and comparison with multiple system atrophy and progressive supranuclear palsy. J Neural Transm Suppl. 1997; 50:9–24. [PubMed: 9120429]

Butterworth RF, Spahr L, Fontaine S, Layrargues GP. Manganese toxicity, dopaminergic dysfunction and hepatic encephalopathy. Metab Brain Dis. 1995; 10:259–267. [PubMed: 8847990]

Cersosimo MG, Koller WC. The diagnosis of manganese-induced parkinsonism. Neurotoxicology. 2006; 27:340–346. [PubMed: 16325915]

Chandra S, Gallardo G, Fernandez-Chacon R, Schluter OM, Sudhof TC. Alpha-synuclein cooperates with CSPalpha in preventing neurodegeneration. Cell. 2005; 123:383–396. [PubMed: 16269331]

Chen MK, Kuwabara H, Zhou Y, Adams RJ, Brasic JR, McGlothan JL, Verina T, Burton NC, Alexander M, Kumar A, Wong DF, Guilarte TR. VMAT2 and dopamine neuron loss in a primate model of Parkinson's disease. J Neurochem. 2008; 105:78–90. [PubMed: 17988241]

Chen MK, Lee JS, McGlothan JL, Furukawa E, Adams RJ, Alexander M, Wong DF, Guilarte TR. Acute manganese administration alters dopamine transporter levels in the non-human primate striatum. Neurotoxicology. 2006; 27:229–236. [PubMed: 16325911]

Couper J. On the effects of black oxide of manganese when inhaled into the lungs. British Annals of Medicine, Pharmacy, Vital Statistics and General Science. 1837; 1:41–42.

Eriksson H, Tedroff J, Thuomas KA, Aquilonius SM, Hartvig P, Fasth KJ, Bjurling P, Langstrom B, Hedstrom KG, Heilbronn E. Manganese induced brain lesions in Macaca fascicularis as revealed by positron emission tomography and magnetic resonance imaging. Arch Toxicol. 1992; 66:403–407. [PubMed: 1444804]

Fabiani G, Rogacheski E, Wiederkehr JC, Khouri J, Cianfarano A. Liver transplantation in a patient with rapid onset parkinsonism-dementia complex induced by manganism secondary to liver failure. Arq Neuropsiquiatr. 2007; 65:685–688. [PubMed: 17876415]

Finkelstein MM, Jerrett M. A study of the relationships between Parkinson's disease and markers of traffic-derived and environmental manganese air pollution in two Canadian cities. Environ Res. 2007; 104:420–432. [PubMed: 17445792]

Fleckenstein AE, Volz TJ, Riddle EL, Gibb JW, Hanson GR. New insights into the mechanism of action of amphetamines. Annu Rev Pharmacol Toxicol. 2007; 47:681–698. [PubMed: 17209801]

Frey KA, Koeppe RA, Kilbourn MR, Vander Borght TM, Albin RL, Gilman S, Kuhl DE. Presynaptic monoaminergic vesicles in Parkinson's disease and normal aging. Ann Neurol. 1996; 40:873–884. [PubMed: 9007092]

Guilarte TR, Chen MK, McGlothan JL, Verina T, Wong DF, Zhou Y, Alexander M, Rohde CA, Syversen T, Decamp E, Koser AJ, Fritz S, Gonczi H, Anderson DW, Schneider JS. Nigrostriatal dopamine system dysfunction and subtle motor deficits in manganese-exposed non-human primates. Exp Neurol. 2006a; 202:381–390. [PubMed: 16925997]

Guilarte TR, McGlothan JL, Degaonkar M, Chen MK, Barker PB, Syversen T, Schneider JS. Evidence for cortical dysfunction and widespread manganese accumulation in the nonhuman primate brain following chronic manganese exposure: a 1H-MRS and MRI study. Toxicol Sci. 2006b; 94:351–358. [PubMed: 16968886]

Guilarte TR, Wagner HN Jr. Frost JJ. Effects of perinatal vitamin B6 deficiency on dopaminergic neurochemistry. J Neurochem. 1987; 48:432–439. [PubMed: 3794715]

Gulson B, Mizon K, Taylor A, Korsch M, Stauber J, Davis JM, Louie H, Wu M, Swan H. Changes in manganese and lead in the environment and young children associated with the introduction of methylcyclopentadienyl manganese tricarbonyl in gasoline--preliminary results. Environ Res. 2006; 100:100–114. [PubMed: 16337847]

Hauser RA, Zesiewicz TA, Rosemurgy AS, Martinez C, Olanow CW. Manganese intoxication and chronic liver failure. Ann Neurol. 1994; 36:871–875. [PubMed: 7998773]

Huang CC, Weng YH, Lu CS, Chu NS, Yen TC. Dopamine transporter binding in chronic manganese intoxication. J Neurol. 2003; 250:1335–1339. [PubMed: 14648150]

Iinuma Y, Kubota M, Uchiyama M, Yagi M, Kanada S, Yamazaki S, Murata H, Okamoto K, Suzuki M, Nitta K. Whole-blood manganese levels and brain manganese accumulation in children receiving long-term home parenteral nutrition. Pediatr Surg Int. 2003; 19:268–272. [PubMed: 12709821]

Ingersoll RT, Montgomery EB Jr. Aposhian HV. Central nervous system toxicity of manganese. II: Cocaine or reserpine inhibit manganese concentration in the rat brain. Neurotoxicology. 1999; 20:467–476. [PubMed: 10385905]

Julian MD, Martin AB, Cuellar B, Rodriguez DF, Navarro M, Moratalla R, Garcia-Segura LM. Neuroanatomical relationship between type 1 cannabinoid receptors and dopaminergic systems in the rat basal ganglia. Neuroscience. 2003; 119:309–318. [PubMed: 12763090]

Kim J, Kim JM, Kim YK, Shin JW, Choi SH, Kim SE, Kim Y. Dopamine transporter SPECT of a liver cirrhotic with atypical parkinsonism. Ind Health. 2007; 45:497–500. [PubMed: 17634700]

Kim Y, Kim JM, Kim JW, Yoo CI, Lee CR, Lee JH, Kim HK, Yang SO, Chung HK, Lee DS, Jeon B. Dopamine transporter density is decreased in parkinsonian patients with a history of manganese exposure: what does it mean? Mov Disord. 2002; 17:568–575. [PubMed: 12112209]

Koerts J, Leenders KL, Koning M, Portman AT, van Beilen M. Striatal dopaminergic activity (FDOPA-PET) associated with cognitive items of a depression scale (MADRS) in Parkinson's disease. Eur J Neurosci. 2007; 25:3132–3136. [PubMed: 17561826]

Lammertsma AA, Hume SP. Simplified reference tissue model for PET receptor studies. Neuroimage. 1996; 4:153–158. [PubMed: 9345505]

Lu CS, Huang CC, Chu NS, Calne DB. Levodopa failure in chronic manganism. Neurology. 1994; 44:1600–1602. [PubMed: 7936281]

Lucchini RG, Albini E, Benedetti L, Borghesi S, Coccaglio R, Malara EC, Parrinello G, Garattini S, Resola S, Alessio L. High prevalence of Parkinsonian disorders associated to manganese exposure in the vicinities of ferroalloy industries. Am J Ind Med. 2007; 50:788–800. [PubMed: 17918215]

Meiri U, Rahamimoff R. Neuromuscular transmission: inhibition by manganese ions. Science. 1972; 176:308–309. [PubMed: 5019787]

Meral H, Kutukcu Y, Atmaca B, Ozer F, Hamamcioglu K. Parkinsonism caused by chronic usage of intravenous potassium permanganate. Neurologist. 2007; 13:92–94. [PubMed: 17351530]

Miller GW, Erickson JD, Perez JT, Penland SN, Mash DC, Rye DB, Levey AI. Immunochemical analysis of vesicular monoamine transporter (VMAT2) protein in Parkinson's disease. Exp Neurol. 1999; 156:138–148. [PubMed: 10192785]

Narita K, Kawasaki F, Kita H. Mn and Mg influxes through Ca channels of motor nerve terminals are prevented by verapamil in frogs. Brain Res. 1990; 510:289–295. [PubMed: 2158851]

Newell KA, Deng C, Huang XF. Increased cannabinoid receptor density in the posterior cingulate cortex in schizophrenia. Exp Brain Res. 2006; 172:556–560. [PubMed: 16710682]

Olanow CW. Manganese-induced parkinsonism and Parkinson's disease. Ann N Y Acad Sci. 2004; 1012:209–223. [PubMed: 15105268]

Paxinos; Huang; Toga. The Rhesus Monkey Brain in Stereotaxic Coordinates. Paxinos, G.; Huang, XF.; Toga, AW., editors. Academic Press; San Diego: 2000. p. 14-114.

Perl DP, Olanow CW. The neuropathology of manganese-induced Parkinsonism. J Neuropathol Exp Neurol. 2007; 66:675–682. [PubMed: 17882011]

Racette BA, McGee-Minnich L, Moerlein SM, Mink JW, Videen TO, Perlmutter JS. Welding-related parkinsonism: clinical features, treatment, and pathophysiology. Neurology. 2001; 56:8–13. [PubMed: 11148228]

Racette BA, Tabbal SD, Jennings D, Good L, Perlmutter JS, Evanoff B. Prevalence of parkinsonism and relationship to exposure in a large sample of Alabama welders. Neurology. 2005; 64:230–235. [PubMed: 15668418]

Rodriguez-Agudelo Y, Riojas-Rodriguez H, Rios C, Rosas I, Sabido PE, Miranda J, Siebe C, Texcalac JL, Santos-Burgoa C. Motor alterations associated with exposure to manganese in the environment in Mexico. Sci Total Environ. 2006; 368:542–556. [PubMed: 16793118]

Santos-Burgoa C, Rios C, Mercado LA, Arechiga-Serrano R, Cano-Valle F, Eden-Wynter RA, Texcalac-Sangrador JL, Villa-Barragan JP, Rodriguez-Agudelo Y, Montes S. Exposure to manganese: health effects on the general population, a pilot study in central Mexico. Environ Res. 2001; 85:90–104. [PubMed: 11161659]

Sari Y, Bell RL, Zhou FC. Effects of chronic alcohol and repeated deprivations on dopamine D1 and D2 receptor levels in the extended amygdala of inbred alcohol-preferring rats. Alcohol Clin Exp Res. 2006; 30:46–56. [PubMed: 16433731]

Schneider JS, Decamp E, Koser AJ, Fritz S, Gonczi H, Syversen T, Guilarte TR. Effects of chronic manganese exposure on cognitive and motor functioning in non-human primates. Brain Res. 2006; 1118:222–231. [PubMed: 16978592]

Shinotoh H, Snow BJ, Chu NS, Huang CC, Lu CS, Lee C, Takahashi H, Calne DB. Presynaptic and postsynaptic striatal dopaminergic function in patients with manganese intoxication: a positron emission tomography study. Neurology. 1997; 48:1053–1056. [PubMed: 9109899]

Stepens A, Logina I, Liguts V, Aldins P, Eksteina I, Platkajis A, Martinsone I, Terauds E, Rozentale B, Donaghy M. A Parkinsonian syndrome in methcathinone users and the role of manganese. N Engl J Med. 2008; 358:1009–1017. [PubMed: 18322282]

Strazielle C, Lalonde R, Amdiss F, Botez MI, Hebert C, Reader TA. Distribution of dopamine transporters in basal ganglia of cerebellar ataxic mice by [^{125}I]RTI-121 quantitative autoradiography. Neurochem Int. 1998; 32:61–68. [PubMed: 9460703]

Surmeier DJ, Ding J, Day M, Wang Z, Shen W. D1 and D2 dopamine-receptor modulation of striatal glutamatergic signaling in striatal medium spiny neurons. Trends Neurosci. 2007; 30:228–235. [PubMed: 17408758]

Takser L, Mergler D, Hellier G, Sahuquillo J, Huel G. Manganese, monoamine metabolite levels at birth, and child psychomotor development. Neurotoxicology. 2003; 24:667–674. [PubMed: 12900080]

Uversky VN, Li J, Fink AL. Metal-triggered structural transformations, aggregation, and fibrillation of human alpha-synuclein. A possible molecular NK between Parkinson's disease and heavy metal exposure. J Biol Chem. 2001; 276:44284–44296. [PubMed: 11553618]

Wolters EC, Huang CC, Clark C, Peppard RF, Okada J, Chu NS, Adam MJ, Ruth TJ, Li D, Calne DB. Positron emission tomography in manganese intoxication. Ann Neurol. 1989; 26:647–651. [PubMed: 2510588]

Wright JA, Brown DR. Alpha-synuclein and its role in metal binding: relevance to Parkinson's disease. J Neurosci Res. 2008; 86:496–503. [PubMed: 17705291]

Yamada M, Ohno S, Okayasu I, Okeda R, Hatakeyama S, Watanabe H, Ushio K, Tsukagoshi H. Chronic manganese poisoning: a neuropathological study with determination of manganese distribution in the brain. Acta Neuropathol. 1986; 70:273–278. [PubMed: 3766127]

Zhou Y, Chen MK, Endres CJ, Ye W, Brasic JR, Alexander M, Crabb AH, Guilarte TR, Wong DF. An extended simplified reference tissue model for the quantification of dynamic PET with amphetamine challenge. Neuroimage. 2006; 33:550–563. [PubMed: 16920365]

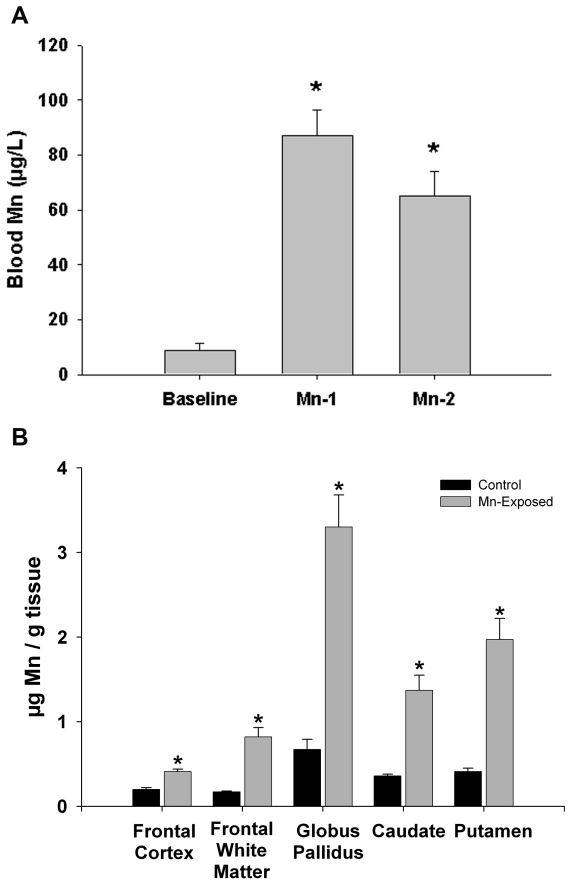

Figure 1.

Blood and brain Mn concentrations in non-human primates. Panel A depicts blood Mn concentrations for the Mn-exposed animals at baseline (prior to Mn administration) and at two time points (Mn-1, 124 ± 12 days; Mn-2, 285 ± 13 days) throughout the Mn dosing period. Panel B depicts brain tissue Mn levels in five different brain regions. Significant accumulation of Mn was observed in all brain areas; however, Mn accumulated to the greatest extent in the globus pallidus. *$p<0.05$, Students *t*-test, relative to baseline (panel A) or control animals (panel B).

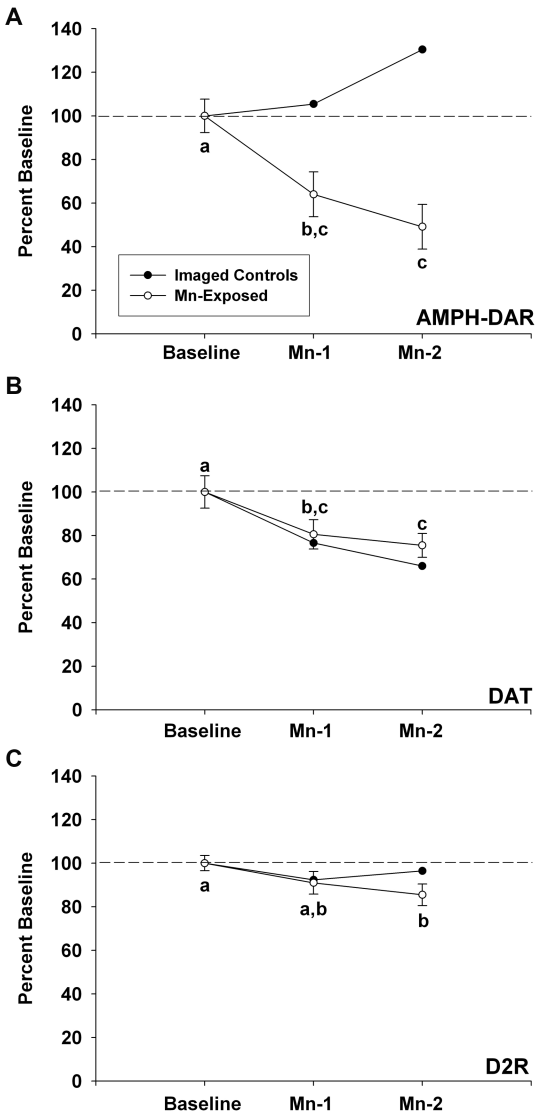

Figure 2.

Results of PET studies in Mn-exposed animals and in imaged-controls. Panel A depicts the PET imaging results for amphetamine-induced dopamine release (AMPH-DAR). Panel B represents the PET imaging results for dopamine transporter (DAT). Panel C describes the PET results for D2 dopamine receptor (D2R) (panel C). Values were normalized to baseline (prior to Mn exposure). For each curve for the Mn-exposed animals, data points with letters in common are not statistically significantly different. Mn exposure produced the most dramatic effect on AMPH-DAR, with a 36% decrease relative to baseline measured at Mn-1 and a 51% decrease measured at Mn-2. This change was not observed in the imaged-controls. Dopamine transporter levels also decreased throughout the dosing period, with a 19.5% decrease observed at Mn-1 and a 24.5% decrease observed at Mn-2. However, these changes tracked with the decreases observed in the imaged-controls, suggesting that the AMPH administered in the PET studies is responsible for the observed decreases in DAT. A decline in D2R of 14.5% reached statistical significance in the Mn-exposed animals by Mn-2.

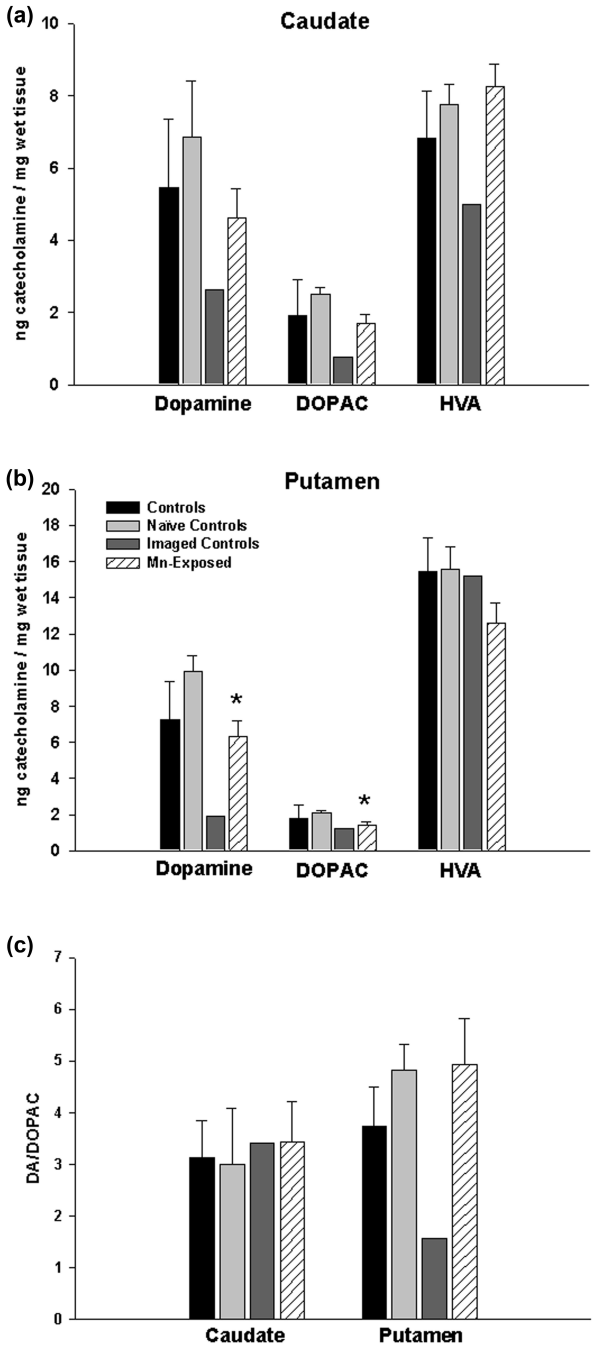

Figure 3.

Brain concentration of dopamine and its metabolites. In the caudate (panel A), neither the levels of dopamine nor its metabolites were different in the Mn-exposed animals relative to the naïve controls. However, the levels of dopamine, DOPAC, and HVA in the caudate were consistently lower in the two imaged-controls compared to the naïve controls and the Mn-exposed animals. In the putamen (panel B), the imaged-controls also showed reduced levels of dopamine and DOPAC relative to the other groups. However, HVA levels were not affected by the procedural administration of AMPH. Dopamine was statistically significantly reduced (*$p<0.05$, Student's *t*-test) by 37% in the putamen of Mn-exposed animals relative to the naïve controls, and DOPAC was significantly reduced by 32%. In

panel C, summary data from panels A and B of the ratio of DA to DOPAC for each treatment group in the caudate and putamen. A reduction in DA/DOPAC was evident only in the putamen of imaged controls. Black bars represent controls (naïve + imaged controls); light grey, naïve controls; dark grey, imaged controls; striped, Mn-exposed. Each value is the mean ± sem of n=6 (controls), n=4 (naïve controls), n=2 (imaged controls), and n=11 (Mn-exposed).

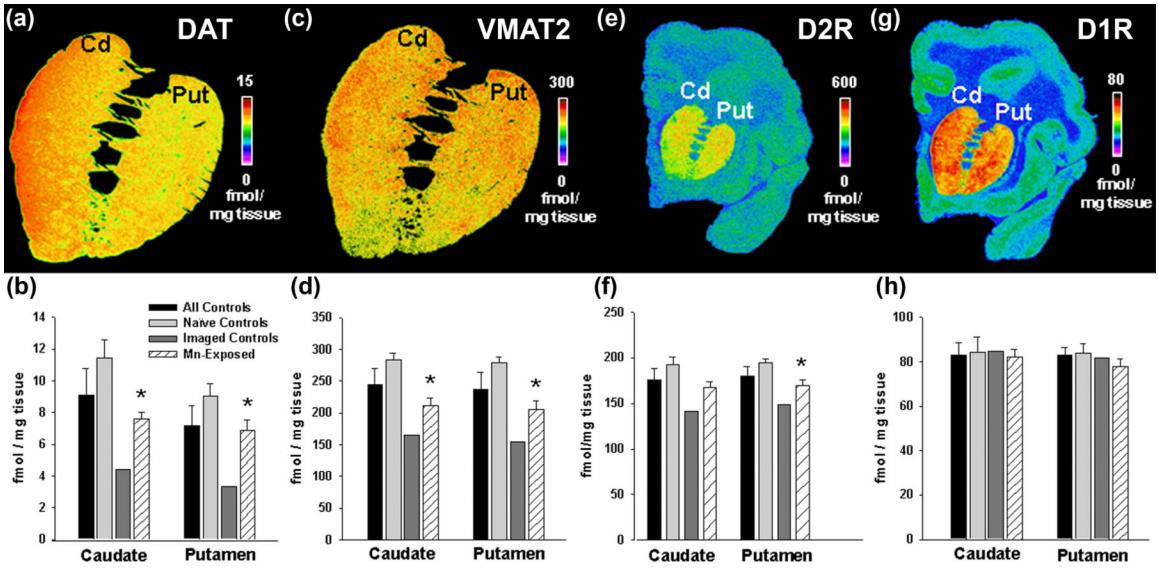

Figure 4.

Quantitative autoradiography of DAT (panels A and B), VMAT2 (panels C and D), D2R (panels E and F), and D1R (panels G and H). Panels A, C, E and G depict a pseudocolor image that shows specific binding of the relevant radioligand in a control animal (animal #123-146) at the rostral level of the caudate and putamen. Below each image (panels B, D, F and H), densitometry is shown for each group of animals. The data shows that DAT and VMAT2 are statistically significantly reduced ($p^* < 0.05$, Student's *t*-test) in the Mn-exposed animals relative to naïve controls in the caudate and putamen. D2R levels in Mn-exposed animals were significantly reduced only in the putamen compared to controls. However, the imaged-controls displayed consistently lower levels of DAT, VMAT2 and D2R than did the Mn-exposed animals. D1 receptor levels did not change in any of the animal groups. Black bars represent controls (naïve + imaged controls); light grey, naïve controls; dark grey, imaged controls; striped, Mn-exposed. Each value is the mean ± sem of n=6 (controls), n=4 (naïve controls), n=2 (imaged controls), and n=8 (Mn-exposed, DAT), n=9 (Mn-exposed, VMAT2), n=11 (Mn-exposed, D1R).

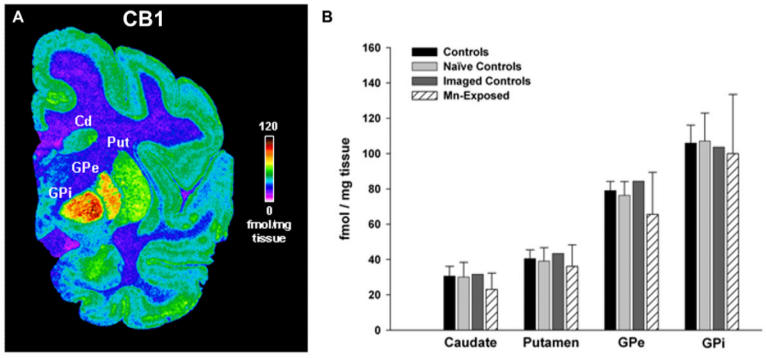

Figure 5.

Quantitative autoradiography of CB1 receptor levels in the caudate, putamen, and the exterior and interior segments of the globus pallidus. Panel A shows a pseudocolor image depicting the level of specific binding of the radioligand to CB1. Panel B shows the quantitative densitometry results. CB1 receptor density is highest in the internal and exterior segments of the globus pallidus relative the caudate, putamen and cortical areas. Chronic Mn-exposure did not affect the levels of CB1 relative to any control group. Each value is the mean ± sem of n=6 (controls), n=4 (naïve controls), n=2 (imaged controls), and n=11 (Mn-exposed), except for the interior segment of the globus pallidus, which has n=10 (Mn-exposed).

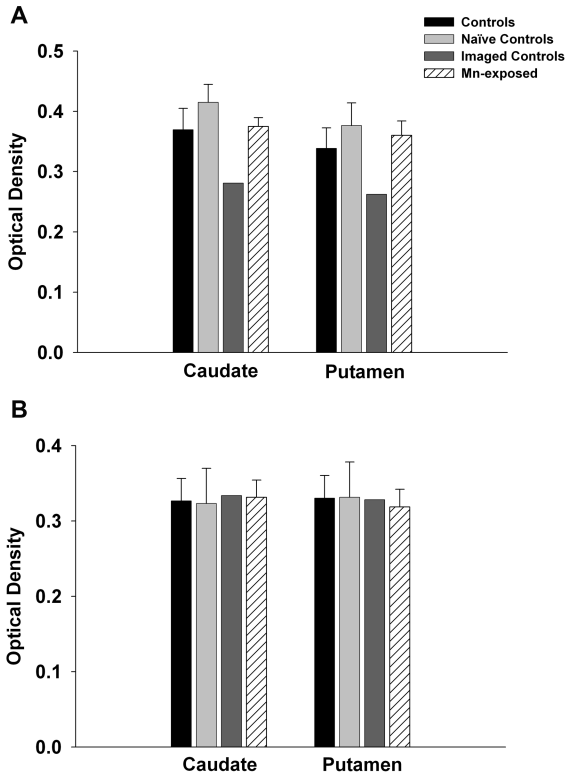

Figure 6.

Tyrosine hydroxylase (TH) and dopamine transporter (DAT) Immunohistochemistry. Panel A shows optical density readings for DAT in the caudate and putamen. Consistent with the autoradiography data, DAT levels were reduced in the imaged-controls that received AMPH only as part of the imaging protocol. However, DAT levels were not affected by chronic Mn exposure. Similarly, neither Mn-exposure nor PET-related AMPH treatment affected TH levels (Panel B). Each value is the mean ± sem of n=6 (controls), n=4 (naïve controls), n=2 (imaged controls), and n=7 (Mn-exposed).

Table 1

Manganese dosing paradigm for non-human primates that received neuroimaging studies. Animals were treated with 3.3-5.0 mg Mn/kg, 5.0-6.7 mg Mn/kg, or 8.3-10.0 mg Mn/kg on a weekly basis for the duration indicated. Injections were given i.v. once per week, except (*) for animals receiving 5.0-6.7 and 8.3-10.0 mg Mn / kg per week, animals were injected with one-half of the weekly Mn dose on two different occasions per week rather than once weekly. Bolus means that the first injection was a single injection and then the dose was split and given on two different occasions per week. Animals #6697, #7426, and #7782 received lower cumulative doses because they developed severe movement abnormalities and Mn dosing was stopped after the Mn-1 imaging set. Six animals that did not receive manganese were used as controls, including four naïve control animals (#6770, #63-111, #123-146, and #123-193) and two imaged-controls (#001-1167, #6499).

Animal ID	Dose Level ($MnSO_4$)	Dose Level (Mn)	Dosing Interval	Exposure Duration (weeks)	Cumulative $MnSO_4$	Cumulative Mn
75W	10-15 mg/kg	3.3-5.0 mg/kg	1/wk	44	455mg/kg	151.7mg/kg
144T	10-15 mg/kg	3.3-5.0 mg/kg	1/wk	50	515mg/kg	171.7mg/kg
107-705	10-15 mg/kg	3.3-5.0 mg/kg	1/wk	42	500mg/kg	166.7mg/kg
3154	10-15 mg/kg	3.3-5.0 mg/kg	1/wk	45	515mg/kg	173.8mg/kg
3114	15-20 mg/kg	5.0-6.7 mg/kg	1/wk	46	635mg/kg	206.4mg/kg
7782	15-20 mg/kg	5.0-6.7 mg/kg	2/wk*	27	435mg/kg	141.4mg/kg
9093	15-20 mg/kg	5.0-6.7 mg/kg	2/wk*	59	770mg/kg	250.8mg/kg
7469	15-20 mg/kg	5.0-6.7 mg/kg	2/wk*	32	525mg/kg	170.7mg/kg
000-8001	15-20 mg/kg	5.0-6.7 mg/kg	2/wk*	34	535mg/kg	173.9mg/kg
001-1099	15-20 mg/kg	5.0-6.7 mg/kg	2/wk*	32	535mg/kg	173.9mg/kg
7839	25-30mg/kg	8.3-10.0 mg/kg	2/wk*	38	640mg/kg	218.3mg/kg
6697	25-30mg/kg	8.3-10.0 mg/kg	Bolus, 2/wk*	7	206mg/kg	68.3mg/kg

Animal ID	Dose Level ($MnSO_4$)	Dose Level (Mn)	Dosing Interval	Exposure Duration (weeks)	Cumulative $MnSO_4$	Cumulative Mn
7426	25-30mg/kg	8.3-10.0 mg/kg	Bolus, 2/wk*	15	340mg/kg	113.3mg/kg